

## Hole-Clump Pair Creation in the Evolution of Energetic-Particle-Driven Geodesic Acoustic Modes

Hao Wang (王灏),<sup>1,\*</sup> Yasushi Todo (藤堂泰),<sup>1,2</sup> and Charlson C. Kim<sup>3</sup>

<sup>1</sup>*The Graduate University for Advanced Studies, Toki 509-5292, Japan*

<sup>2</sup>*National Institute for Fusion Science, Toki 509-5292, Japan*

<sup>3</sup>*FAR-TECH, Inc., San Diego, California 92121-1136, USA*

(Received 5 September 2012; published 12 April 2013)

Nonlinear frequency chirping of the energetic-particle-driven geodesic acoustic mode (EGAM) is investigated using a hybrid simulation code for energetic particles interacting with a magnetohydrodynamic fluid. It is demonstrated in the simulation result that both frequency chirping up and chirping down take place in the nonlinear evolution of the EGAM. It is found that two hole-clump pairs are formed in the energetic particle distribution function in two-dimensional velocity space of pitch angle variable and energy. One pair is formed in the phase space region that destabilizes the instability, while the other is formed in the stabilizing region. The transit frequency of the hole (clump) in the destabilizing region chirps up (down), while in the stabilizing region the hole (clump) chirps down (up). The transit frequencies of particles in the holes and clumps are in good agreement with the chirping EGAM frequency indicating that the particles are kept resonant with the EGAM during the nonlinear frequency chirping. Continuous energy transfer takes place from the destabilizing phase space region to the stabilizing region during the spontaneous frequency chirping of the wave.

DOI: [10.1103/PhysRevLett.110.155006](https://doi.org/10.1103/PhysRevLett.110.155006)

PACS numbers: 52.35.Fp, 52.55.Hc, 52.65.Ww

The geodesic acoustic mode (GAM) is an oscillatory zonal flow coupled with density and pressure perturbations in toroidal plasmas [1–3]. Recently, an energetic-particle-driven GAM (EGAM) and the associated frequency chirping were observed at JET [4,5], DIII-D [6], and LHD [7,8]. It was theoretically and computationally demonstrated that energetic particles induce an EGAM with a global spatial profile and spatially uniform frequency despite the local GAM frequency's dependence on temperature and safety factor [9]. Theoretical studies have been made on the fast excitation due to the loss boundary in pitch angle [10], on the coupling to the GAM continuum [11], on the nonlinear second harmonics of the EGAM [12], and on the energy channeling from energetic particles to thermal ions through EGAM [13]. In the DIII-D experiment, drops in neutron emission follow the EGAM bursts suggesting beam ion losses. Understanding the EGAM is important for magnetic confinement fusion where the energetic particles need to be well confined for the bulk plasma heating.

The frequency chirping of the EGAM observed at JET is attributed to the formation of a hole-clump pair in energetic particle phase space [5]. The spontaneous creation of holes and clumps in phase space was discovered by computer simulation for both destabilizing and stabilizing particle species [14,15]. The theory of the associated frequency chirping is also presented in Refs. [14,15]. The spontaneous frequency chirping takes place for both the assumed constant mode damping and the self-consistent damping due to heavy stabilizing species. Comprehensive simulation studies have been devoted to the nonlinear evolution of the bump-on-tail problem including the hole-clump pair

creation [16–18]. The frequency chirping of an energetic particle mode and Alfvén eigenmodes in tokamak plasmas have been investigated by computer simulations, and the relation between the frequency chirping and the hole-clump pair creation has been discussed [19,20].

However, the computational demonstration of the hole-clump pair creation has so far been limited to the bump-on-tail problem in one-dimensional velocity space. It is not straightforward to find such a phase space structure in toroidal plasmas, because a huge number of computational particles or phase space grid points is needed to resolve five-dimensional phase space (three dimensions for configuration space and two dimensions for velocity space), and both the particle energy and the canonical momentum evolve during the interaction with the wave. Since the axisymmetry of the EGAM reduces phase space to four dimensions and conserves toroidal canonical momentum, the EGAM is an interesting subject of the phase space structure study. In this Letter, both chirping up and chirping down of the EGAM frequency are reproduced by simulation and the phase space structure of the energetic particles is investigated.

A hybrid simulation code for energetic particles interacting with a magnetohydrodynamic (MHD) fluid, MEGA [21,22], is used for the simulation of the EGAM. In the MEGA code, the bulk plasma is described by the nonlinear MHD equations. The drift kinetic description and the  $\delta f$  particle method are applied to the energetic particles. The physics condition in the simulation is based on a LHD experiment [8],  $B_0 = 1.5$  T, electron density  $n_e = 0.1 \times 10^{19} \text{ m}^{-3}$ , electron temperature at the magnetic axis

$T_e = 4$  keV, and bulk plasma beta value at the magnetic axis equal to  $7.2 \times 10^{-4}$ . The neutral beam injection energy is  $E_{\text{NBI}} = 170$  keV. Since the kinetic GAM frequency at LHD is close to those in tokamaks [3], a tokamak type equilibrium is examined with concentric magnetic surfaces, and with the safety factor profile and the aspect ratio similar to the LHD plasma. The safety factor  $q$  profile is a weak shear profile with  $q = 2.0$  at the magnetic axis and  $q = 0.83$  at the plasma edge. The major radius of the magnetic axis is  $R_0 = 3.9$  m and the plasma minor radius is  $a = 0.65$  m. Cylindrical coordinates  $(R, \phi, z)$  are employed for the simulation with numbers of grid points (128, 16, 128), respectively, although the equilibrium and the fluctuations do not depend on  $\phi$ . The number of the computational particles is 2 million.

The equilibrium energetic particle distribution function  $f_0$  can be written using constants of motion as

$$f_0 = f_0(E, \mu, P_\phi, \sigma), \quad (1)$$

$$P_\phi = Z_h e \psi + R m v_{\parallel} b_\phi, \quad (2)$$

where  $E$  is the particle energy,  $\mu$  is the magnetic moment,  $P_\phi$  is the toroidal canonical momentum,  $\sigma$  distinguishes the orbit types (with  $\sigma = 1$  for copassing particles,  $\sigma = 0$  for trapped particles, and  $\sigma = -1$  for counterpassing particles).  $Z_h e$  and  $m$  are the particle charge and mass,  $\psi$  is the poloidal magnetic flux,  $v_{\parallel}$  is the parallel velocity, and  $b_\phi$  is the toroidal component of the magnetic field unit vector.

Assuming the separation of variables, Eq. (1) is expressed by

$$f_0 = f_0(E, \mu, P_\phi, \sigma) = \mathcal{G}(E) \mathcal{H}(\Lambda) I(E, \mu, P_\phi, \sigma), \quad (3)$$

where  $\Lambda = \mu B_0 / E$  is the pitch angle variable with the  $B_0$  magnetic field strength at the magnetic axis. The energy distribution  $\mathcal{G}(E)$  is a slowing down distribution. The function  $\mathcal{H}(\Lambda)$  is introduced to model anisotropic distributions in pitch angle  $\mathcal{H}(\Lambda) = \exp[-(\Lambda - \Lambda_{\text{peak}})^2 / \Delta\Lambda^2]$ , where the  $\Lambda_{\text{peak}}$  represents the pitch angle for the distribution peak and  $\Delta\Lambda$  is a parameter to control the distribution width. In the present simulation,  $\Lambda_{\text{peak}} = 0.3$  and  $\Delta\Lambda = 0.2$ . The function  $I$  represents the radial profile which is consistent with the energetic particle beta profile

$$I(E, \mu, P_\phi, \sigma) = \exp(-\psi_{\text{nrn}} / \xi^2), \quad (4)$$

$$\psi_{\text{nrn}} = 1 - \frac{P_\phi - \sigma R_0 m v_0}{Z_h e \psi_{\text{max}}}, \quad (5)$$

where  $v_0 = \sqrt{2(E - \mu B_{\text{min}}) / m}$ ,  $\psi_{\text{max}}$  is the maximum value of  $\psi$ , and  $\xi = 0.5$  in the present simulation.

The time derivative of  $\delta f = f - f_0$  at each marker particle is given by

$$\frac{d}{dt} \delta f = \frac{d}{dt} (f - f_0) = -\frac{dE}{dt} \frac{\partial f_0}{\partial E} - \frac{dP_\phi}{dt} \frac{\partial f_0}{\partial P_\phi}. \quad (6)$$

The destabilization of the EGAM arises from the energy derivative of  $f_0$  with the most important contribution from the second term of the equation below.

$$\frac{\partial f_0}{\partial E} = \frac{\partial \mathcal{G}}{\partial E} \mathcal{H} I + \mathcal{G} \frac{\partial \Lambda}{\partial E} \frac{\partial \mathcal{H}}{\partial \Lambda} I + \mathcal{G} \mathcal{H} \frac{\partial I}{\partial E}. \quad (7)$$

The initial energetic particle distribution function in velocity space is shown in Fig. 1(a). The dashed curves represent constant  $\mu$ , and particles evolve only along the dashed curves because  $\mu$  is an adiabatic invariant. In area A,  $\frac{\partial f}{\partial E}|_{\mu=\text{const}} > 0$ , and the particles with positive  $\frac{\partial f}{\partial E}$  can destabilize the EGAM. In area B,  $\frac{\partial f}{\partial E}|_{\mu=\text{const}} < 0$ , and particles in this area stabilize the EGAM. Figure 1(b) shows the energy transfer rate from the EGAM to energetic particles in  $(\Lambda, E)$  space in the linear phase. The purple color represents negative energy transfer, which means the energy transfer from particles to the EGAM, destabilizing the mode. In contrast, the red color represents positive energy transfer that stabilizes the mode. The energy transfer rate in the destabilizing region is higher than that in the stabilizing region. Then, the EGAM is excited on the whole. Notice that the purple region in Fig. 1(b) is located in area A in Fig. 1(a), and the red region in Fig. 1(b) is located in area B in Fig. 1(a). These two figures are consistent with each other, clarifying the mode destabilization mechanism.

The EGAM frequency chirping takes place in the non-linear phase, and the evolution of the frequency spectrum and the poloidal velocity is shown in Fig. 2. The mode

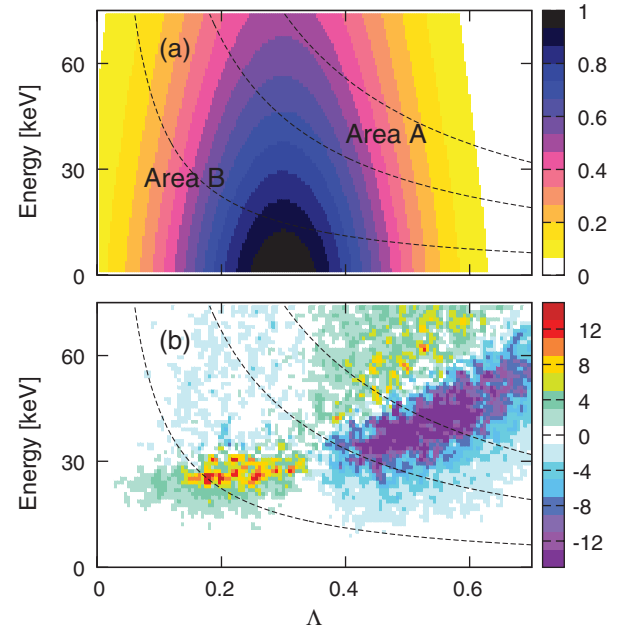


FIG. 1 (color). Panel (a) shows the normalized initial energetic particle distribution in  $(\Lambda, E)$  space, and panel (b) shows the energy transfer rate from the EGAM to energetic particles. Dashed curves represent constant  $\mu$ .

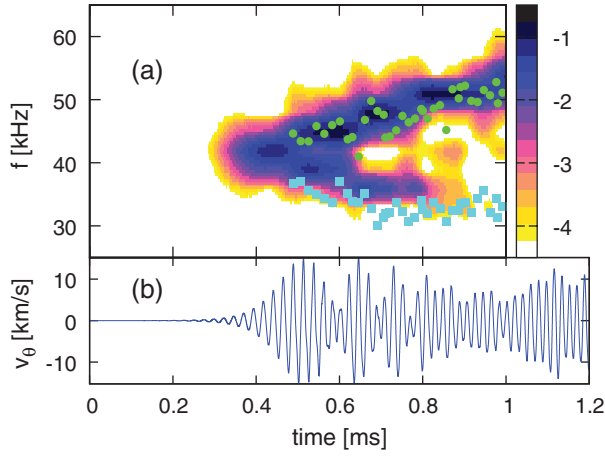


FIG. 2 (color). Time evolution of (a) the EGAM frequency spectrum and (b) the poloidal velocity  $v_\theta$ . Both panels share the horizontal axis. The color bar indicates the magnitude in logarithmic scale. Green dots and cyan squares plotted in panel (a) represent transit frequencies of the hole and clump, respectively, that are analyzed along the  $\mu = 15$  keV/T curve.

frequency chirps up from 40 to 50 kHz in 0.4 ms. Another branch chirps down, but this branch is weaker than the chirping up branch. The energetic particle  $\delta f$  distribution in two-dimensional velocity space  $(\Lambda, E)$  is shown for  $t = 0.51$  ms, 0.80 ms, and 1.02 ms in Figs. 3(a)–3(c), where the blue color represents  $\delta f < 0$  (hole) while the red color represents  $\delta f > 0$  (clump). The  $\delta f$  distribution is integrated over the whole simulation domain. We see in the figure that two pairs of hole and clump are created along the constant  $\mu$  curves in  $(\Lambda, E)$  space. One pair is created along the higher- $\mu$  curve with a hole in the high energy side and a clump in the low energy side. Note that this pair is created in the region destabilizing the instability labeled as Area A in Fig. 1(a). This pair is consistent with the Berk-Breizman model where a hole (clump) is created in the high (low) energy side. The other pair is created along the lower- $\mu$  curve in the stabilizing region Area B in Fig. 1(a). We see a clump in the high energy side and a hole in the low energy side. This is the first discovery of the creation of a hole-clump pair in the stabilizing region in phase space. The solid curves in Figs. 3(a)–3(c), represent the constant poloidal transit frequency defined by  $f_{tr} = \sqrt{1 - \Lambda v} / (2\pi q R_0)$ , where  $v$  is the particle velocity and  $q$  is the safety factor value. The resonance condition between an energetic particle and the EGAM is given by  $f_{EGAM} = f_{tr}$ . If the transit frequency is in agreement with the EGAM frequency, the particle is resonant with the EGAM. The particle energy can evolve during the interaction with the EGAM, moving across the solid curves in Figs. 3(a)–3(c). At  $t = 0.51$  ms, as shown in Fig. 3(a), the transit frequency of the right hole (or the hole with higher  $\mu$  value) is around 45 kHz. At  $t = 0.80$  ms as shown in Fig. 3(b), the hole shifts upward along the dashed curve (constant  $\mu$  curve), and the transit frequency becomes close to 50 kHz. At

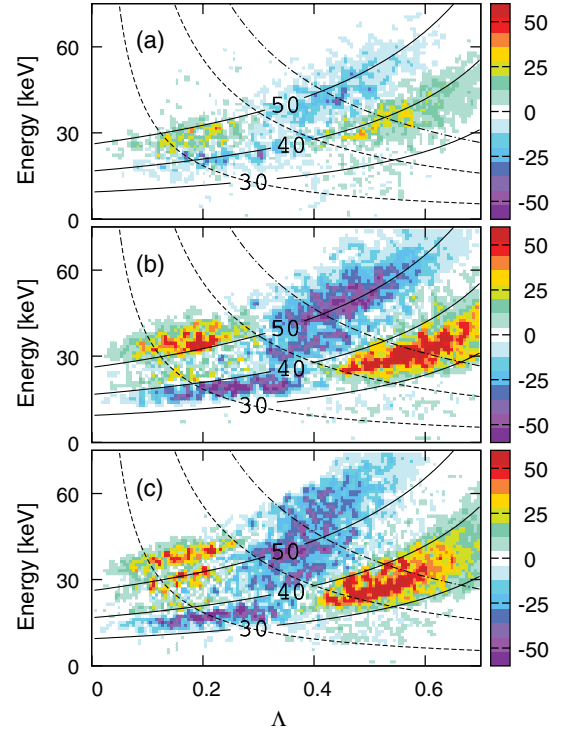


FIG. 3 (color). Energetic particle  $\delta f$  distribution in  $(\Lambda, E)$  space at (a)  $t=0.51$  ms, (b)  $t=0.80$  ms, and (c)  $t=1.02$  ms. Solid curves represent constant  $f_{tr}$  with the values (kHz) labeled in the figure, and dashed curves represent constant  $\mu$  (the dot-dashed curves represent  $\mu = 15$  keV/T).

$t = 1.02$  ms as shown in Fig. 3(c), the transit frequency of the hole exceeds 50 kHz. Similarly, the left clump (or the clump with the lower  $\mu$  value) is also shifting upward along the dashed curve, and the transit frequency increases. The transit frequencies of the right hole and left clump are increasing, and they correspond to the chirping up branch in Fig. 2. On the other hand, the left hole and right clump (or the hole with the lower  $\mu$  and the clump with the higher  $\mu$ ) shift to lower transit frequency. The left hole and right clump correspond to the chirping down branch in Fig. 2. For a more accurate comparison of the transit frequency with the EGAM frequency, the perturbative distribution  $\delta f$  is analyzed as a function of transit frequency along the  $\mu = 15$  keV/T curve [the dot-dashed curve in Figs. 3(a)–3(c)]. The particles with  $14.25$  keV/T  $\leq \mu \leq 15.75$  keV/T are investigated. The transit frequencies of the peak (= clump) and the bottom (= hole) of the perturbative distribution are mapped into Fig. 2(a). We see good agreement between the EGAM frequencies and the transit frequencies of the hole and the clump. This indicates that the particles comprising the hole and clump are kept resonant with the EGAM during the frequency chirping.

In the hole-clump creation found in Ref. [15], the value of the total distribution function  $f = f_0 + \delta f$  in the hole and clump is kept constant at the value where the linear instability takes place. We have investigated  $f$  following

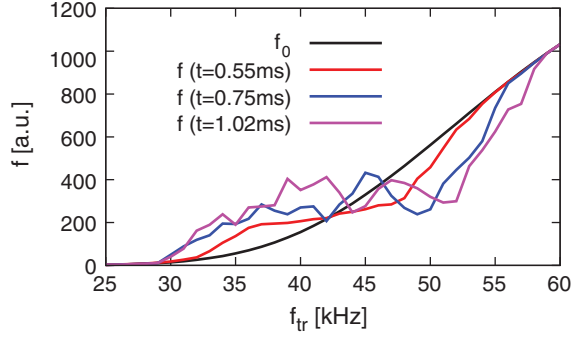


FIG. 4 (color). Total distribution  $f = f_0 + \delta f$  as a function of transit frequency.

the particle with the maximum  $|\delta f|$  ( $\delta f < 0$ ) at  $t = 1.02$  ms. We use the particle as a tracer of the hole. The total distribution  $f$  is analyzed in a phase space region that contains the tracer particle and is bounded within a range of  $\pm 5\%$  for the magnetic moment,  $\pm 9\%$  for the toroidal canonical momentum, and  $\pm \pi/8$  for the geometrical poloidal angle. The central value of the magnetic moment is 16 keV/T for this analysis. Figure 4 shows the total distribution  $f = f_0 + \delta f$  as a function of transit frequency for different times where each distribution is averaged over 0.02 ms. We see that the value of  $f$  at the bottom of the hole is kept roughly constant in time, and that the hole propagates towards higher transit frequency. This is consistent with the results presented in Ref. [15]. Though the analysis is focused on the hole, we also see clump formation in the lower transit frequency. The termination of the clump frequency shift after  $t \sim 0.7$  ms can be attributed to the weak gradient of  $f_0$  for  $f_{tr} \leq 35$  kHz.

In order to fully investigate the relation between the EGAM frequency and the transit frequency of hole-clump pairs, we investigate the transit frequency evolution of particles in the holes and clumps. For this investigation, we executed another run with numbers of grid points (64, 16, 64) and a half million computational particles for the same physics condition as in the standard run we have discussed in this Letter. Figure 5 shows the transit frequency evolution of particles in the holes and clumps for (a) the stabilizing region and (b) the destabilizing region with the EGAM frequency spectrum evolution. We see that the EGAM frequency chirping is similar to that shown in Fig. 2. Black curves represent the transit frequency evolution of particles in the holes, and green curves that in the clumps. We see good agreement between the transit frequency and the EGAM frequency during the frequency chirping. This clearly demonstrates that the particles in the holes and clumps are kept resonant with the EGAM. It is interesting to note that in the stabilizing region shown in Fig. 5(a) the transit frequency for the clump (hole) chirps up (down). Energy is continuously transferred from the hole and clump in the destabilizing

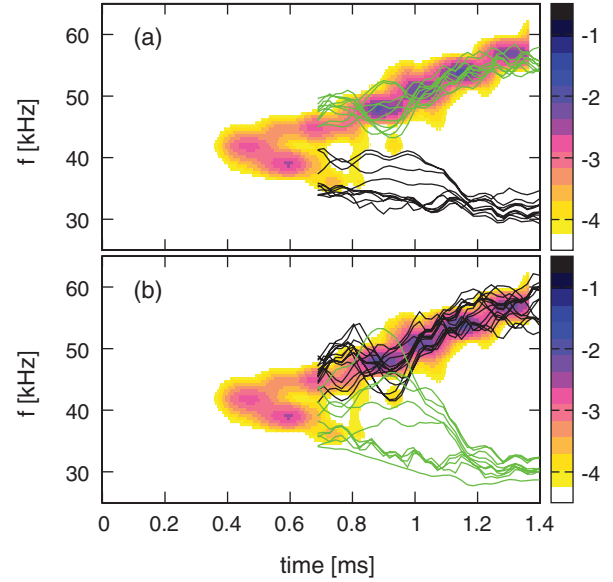


FIG. 5 (color). Time evolution of the EGAM power spectrum. The black curves represent the transit frequency evolution of particles in the holes, and the green curves represent that in the clumps for (a) the stabilizing phase space region and (b) the destabilizing region.

region to those in the stabilizing region during the frequency chirping.

The double phase space structure formation was first discovered in Ref. [15] for light destabilizing and heavy stabilizing species in one-dimensional velocity space. It is interesting to note that the frequency chirping rate in Figs. 3 and 5 looks constant in time. Such a constant frequency chirping rate is consistent with the results presented in Ref. [15]. On the other hand, Ref. [15] predicts that the trapping frequency of the stabilizing species is lower than that of the destabilizing species for the double phase space structure formation. The oscillations in transit frequency of the resonant particles in Fig. 5 may represent the trapping by the wave. We do not see any significant difference in the oscillation frequency between (a) stabilizing and (b) destabilizing particles.

In summary, we have carried out the nonlinear simulations of the EGAM, and have found that spontaneous frequency chirping takes place and two hole-clump pairs are formed in the energetic particle distribution function in two-dimensional velocity space of pitch angle variable and energy. One pair is formed in the phase space region that destabilizes the instability, while the other is formed in the stabilizing region. The transit frequencies of particles in the holes and clumps are in good agreement with the chirping EGAM frequency indicating that the particles are kept resonant with the EGAM during the nonlinear frequency chirping. We would like to emphasize that we have found the hole-clump pairs in a more realistic system

than that investigated in Ref. [15]. Our results indicate that the double phase space structure of stabilizing and destabilizing particles is ubiquitous for the spontaneous frequency chirping phenomena.

Numerical computations were performed at the Plasma Simulator of the National Institute for Fusion Science. This work was supported by the NIFS Collaborative Research Program (NIFS11KNST018). The authors thank Professor B. N. Breizman, Professor T. Ido, Professor M. Osakabe, Professor T.-H. Watanabe, Professor H. Sugama, Dr. K. Ogawa, and Dr. W. Chen for fruitful discussions.

---

\*wanghao@nifs.ac.jp

- [1] N. Winsor, J. L. Johnson, and J. M. Dawson, *Phys. Fluids* **11**, 2448 (1968).
- [2] P. H. Diamond, S.-I. Itoh, K. Itoh, and T. S. Hahm, *Plasma Phys. Controlled Fusion* **47**, R35 (2005).
- [3] H. Sugama and T.-H. Watanabe, *Phys. Plasmas* **13**, 012501 (2006).
- [4] C. Boswell, H. Berk, D. Borba, T. Johnson, S. Pinches, and S. Sharapov, *Phys. Lett. A* **358**, 154 (2006).
- [5] H. Berk, C. Boswell, D. Borba, A. Figueiredo, T. Johnson, M. Nave, S. Pinches, S. Sharapov, and JET EFDA contributors, *Nucl. Fusion* **46**, S888 (2006).
- [6] R. Nazikian, G. Y. Fu, M. E. Austin, H. L. Berk, R. V. Budny, N. N. Gorelenkov, W. W. Heidbrink, C. T. Holcomb, G. J. Kramer, G. R. McKee, M. A. Makowski, W. M. Solomon, M. Shafer, E. J. Strait, and M. A. Van Zeeland, *Phys. Rev. Lett.* **101**, 185001 (2008).
- [7] K. Toi *et al.*, *Phys. Rev. Lett.* **105**, 145003 (2010).
- [8] T. Ido *et al.*, the LHD Experiment Group, *Nucl. Fusion* **51**, 073046 (2011).
- [9] G. Y. Fu, *Phys. Rev. Lett.* **101**, 185002 (2008).
- [10] H. L. Berk and T. Zhou, *Nucl. Fusion* **50**, 035007 (2010).
- [11] Z. Qiu, F. Zonca, and L. Chen, *Plasma Phys. Controlled Fusion* **52**, 095003 (2010).
- [12] G. Y. Fu, *J. Plasma Phys.* **77**, 457 (2011).
- [13] M. Sasaki, K. Itoh, and S.-I. Itoh, *Plasma Phys. Controlled Fusion* **53**, 085017 (2011).
- [14] H. Berk, B. Breizman, and N. Petviashvili, *Phys. Lett. A* **234**, 213 (1997); **238**, 408 (1998).
- [15] H. L. Berk, B. N. Breizman, J. Candy, M. Pekker, and N. V. Petviashvili, *Phys. Plasmas* **6**, 3102 (1999).
- [16] R. G. L. Vann, R. O. Dendy, and M. P. Gryaznevich, *Phys. Plasmas* **12**, 032501 (2005).
- [17] M. Lesur, Y. Idomura, and X. Garbet, *Phys. Plasmas* **16**, 092305 (2009).
- [18] M. K. Lilley, B. N. Breizman, and S. E. Sharapov, *Phys. Plasmas* **17**, 092305 (2010).
- [19] Y. Todo, K. Shinohara, M. Takechi, and M. Ishikawa, *J. Plasma Fusion Res.* **79**, 1107 (2003).
- [20] S. D. Pinches, H. L. Berk, M. P. Gryaznevich, and S. E. Sharapov, JET-EFDA Contributors, *Plasma Phys. Controlled Fusion* **46**, S47 (2004).
- [21] Y. Todo and T. Sato, *Phys. Plasmas* **5**, 1321 (1998).
- [22] Y. Todo, *Phys. Plasmas* **13**, 082503 (2006).